Hindawi
Journal of Sensors
Volume 2017, Article ID 3280691, 13 pages
https://doi.org/10.1155/2017/3280691

Research Article

Methodology for Thermal Behaviour Assessment of Homogeneous Façades in Heritage Buildings

Enrique Gil,[1] Carlos Lerma,[2] Jose Vercher,[2] and Ángeles Mas[2]

[1]*Department of Structural Construction, Universitat Politècnica de València, Camino de Vera, s/n, 46022 Valencia, Spain*
[2]*Department of Architectural Constructions, Universitat Politècnica de València, Camino de Vera, s/n, 46022 Valencia, Spain*

Correspondence should be addressed to Carlos Lerma; clerma@csa.upv.es

Received 7 April 2017; Accepted 2 July 2017; Published 27 July 2017

Academic Editor: Carlota M. Grossi

It is fundamental to study the thermal behaviour in all architectural constructions throughout their useful life, in order to detect early deterioration ensuring durability, in addition to achieving and maintaining the interior comfort with the minimum energy consumption possible. This research has developed a methodology to assess the thermal behaviour of façades in heritage buildings. This paper presents methodology validation and verification (V & V) through a laboratory experiment. Guidelines and conclusions are extracted with the employment of three techniques in this experiment (thermal sensors, thermal imaging camera, and 3D thermal simulation in finite element software). A small portion of a homogeneous façade has been reproduced with indoor and outdoor thermal conditions. A closed chamber was constructed with wood panels and thermal insulation, leaving only one face exposed to the outside conditions, with a heat source inside the chamber that induces a temperature gradient in the wall. With this methodology, it is possible to better understand the thermal behaviour of the façade and to detect possible damage with the calibration and comparison of the results obtained by the experimental and theoretical techniques. This methodology can be extrapolated to the analysis of the thermal behaviour of façades in heritage buildings, usually made up of homogeneous material.

1. Introduction

In order to optimize the available energy resources, it is necessary to analyse the buildings energy consumption, since the building industry has a significant weight in the consumption of resources (energy and raw materials). Thermal response of the enclosures is a very important factor in this regard. On the other hand, the thermal study of a façade can give information regarding its pathological state. This paper develops a methodology that analyses heritage building façades in a thermal way with a low economic cost.

It is necessary to consider multiple constructive and environmental factors in thermal response of façades and in energy losses that occur through them. Constructive design of façades and possible pathology or alteration of the building materials are the most important factors. A correct arrangement of the façade layers and good carpentry are highlighted among the constructive factors. Green urban infrastructures [1] that contribute to heat mitigation [2] and to reducing ambient temperature and improving thermal comfort [1, 3, 4] stand out among the environmental factors. The design of roofs and green walls also influences the boundary climatic conditions [5–7]. The density of green areas affects the incidence and absorption of solar radiation, which induces a lower surface temperature [8].

Every day there is greater interest in collecting data from buildings [9] to better understand and improve knowledge of energy use [10] and thermal comfort [11].

Some failures in building envelope occur often during the construction process [12–14]. In historic buildings, most faults occur during their service life, so it is recommendable to monitor them.

The deterioration monitoring would give an early warning of incipient problems that allow the planning of the maintenance programs, minimizing the relevant costs [15, 16]. In fact, an analysis of statistical data can be performed to obtain valuable information for preventive conservation [17]. Preventive conservation consists of a working method and a

combination of techniques that help to determine and control the deterioration process of cultural heritage in order to take the necessary actions before it occurs [18].

The use of data monitoring systems together with improved service-life prediction models leads to additional savings in life cycle costs [19, 20]. The development of new sensor concepts allows for a more rational approach to the assessment of repair options and scheduling of inspection and maintenance programmes [20] in traditional buildings or other types of structures.

To facilitate more cost-effective data collection for a wide variety of important building environmental and operational parameters is necessary to search tools [21] with an affordable price. They also have to be easy to build and customize according to the needs of each case, and they can store lots of data with a reasonable accuracy. This research work combines three techniques: thermal sensors, thermography, and finite elements simulation.

On the one hand, a low-cost Arduino-based microcontroller has been employed in this research, because it is a cheap, flexible, and programmable open-source system, with easy-to-use hardware and software components [21, 22]. This microcontroller has been used as an interface to receive information from sensors and as a data-logger. Also, it activates or deactivates the heat source of the specimen according to the temperature recorded by the sensors. An exhaustive study has never been done to know the thermal flow with low-cost sensors, although this type of microcontroller has already been used by environmentalists with sensors [23–25].

On the other hand, there are several modalities [26] in the use of infrared technology, but the most common ones are active thermography, which consists of artificially heating the sample, and passive thermography, where the material or enclosure is heated by the natural effect of the solar energy. The best option is passive thermography when large surfaces are studied because it fits the real situation very well [27], for example, the façades of buildings, especially if they are located in an urban environment where the streets are narrow. Passive thermography has also been used to assess the effect of leakage points in buildings [28].

Nondestructive techniques such as temperature sensors and thermography facilitate the study of building materials without damaging the building, especially its façades. Most historic buildings have been built with different types of stone. Usually, these types of buildings have thick façades composed of one or two materials. In the case of stone walls, this material covered the entire thickness of the wall. Different materials can be alternated, as, for example, the case of brick with earth or rammed earth walls, if the façade was formed by other materials. The state of deterioration of a stone monument is characterised by the type, intensity, and extent of the damage. Determining the location of the forms of deterioration has been demonstrated to be a highly appropriate research method for preventive conservation.

Thermography may propose some difficulties if a quantitative approach is intended [29], but in this work, it is combined with two other techniques, allowing in this way locating and quantifying the magnitude of damage.

The main objective of this research is to develop a specimen in the laboratory that allows obtaining real data. The specimen consists in generating a thermal flow through a homogeneous stone material. Temperature data were recorded using Arduino-based software and hardware designed by the authors. Temperatures are confronted with thermographic technology. Finally, the data obtained help to calibrate and verify a three-dimensional model of finite elements, which allows obtaining a greater amount of data and a more global estimate of the thermal behaviour. From this specimen, this work proposes a methodology to evaluate the thermal behaviour of façades in historic buildings and to detect pathology.

2. Materials and Methods

This research presents a methodology applicable to any material and historical building with the objective of evaluating its envelope thermally.

The methodology presented in this paper uses three techniques. One technique gives theoretical results and the other two obtain real and experimental results. The first technique is based on the elaboration of a finite element model with simulation software. This gives the theoretical results of the experiment, that is, the temperature reached by the material at each point with current conditions if it were homogeneous and it had no damage or failures. One of the techniques that provides experimental results is the use of temperature sensors that record the temperature data along the thickness of the façade. And the other experimental technique used is the thermal camera, which allows mapping temperatures on the exterior surfaces. The methodology basically consists of analysing the variation of temperature data obtained theoretically and experimentally. If the data are very similar, the façade is healthy. However, if the data change significantly in any area, there is pathology. This paper shows practical examples to understand the detection of cracks, mass faults, detachments, and so on.

2.1. Design of the Specimen Tested. A façade specimen, a model, has been constructed to develop this research.

The model is a box of $73 \times 63 \times 36\,\text{cm}^3$. The exterior is made of chipboard that allows rigid and stable walls. A solid light concrete block has been placed inside the box. This block is $25 \times 25 \times 60\,\text{cm}^3$ and it is wrapped by thermal insulation of rock wool 4 cm thick, except on two of its faces. The heat flows from the inside of the box to the outside through the block of lightweight concrete. The characteristics of the materials used can be seen in Table 1. Thus, a closed and isolated chamber has been built, with the heat source simulating the conditions inside the building (Figures 1 and 2). Up to 11 thermometers have been placed inside the wooden box and inside the solid light concrete block. The heat source has been a single 60 W bulb in this case.

A piece of rock wool has been placed inside the air chamber between the heat source and the concrete block. This piece is in the central third in the plan view. This is done to avoid direct radiation to the block and, in this way, only the physical phenomena of conduction and convection

Table 1: Properties of the used materials.

ID material	Material	Density (Kg/m^3)	Specific heat ($J/Kg^{\circ}K$)	Thermal conductivity ($W/m^{\circ}K$)
#1	Chipboard	750	1600	0.24
#2	Rock wool	40	800	0.035
#3	Solid light concrete block	400	1000	0.1

Table 2: Temperature sensors used.

#	Type	Observations
T01	DS18B20	Outside temperature.
T02	DS18B20	Outside film coefficient temperature.
T03	DS18B20	Outside edge temperature (top).
T04	DS18B20	Outside edge temperature (bottom).
T05	K	5 cm from outside edge temperature.
T06	DS18B20	Intermediate zone temperature.
T07	K	5 cm from inside edge temperature.
T08	DS18B20	Inside edge temperature.
T09	DS18B20	Inside film coefficient temperature.
T10	DS18B20	Inside temperature (up).
T11	DS18B20	Inside temperature (bottom, protected from the source). It controls the heat source's on/off switching.

Figure 1: Specimen to perform the specimen without the top cover.

will appear. These two phenomena appear in the envelopes of buildings.

Table 2 summarizes the positions of each thermometer. Up to 11 temperature sensors have been placed from the heated interior chamber to the outer space at ambient temperature. Thus, the temperature reached by the air, in the interior and in the outside, can be known at any moment. Also, the temperature reaches the homogeneous material in the most prominent points: near the edges and in the central part.

It is noteworthy that the indoor sensors T9, T10, and T11 have been protected against the heat source, since it also radiates infrared energy that skews the temperature reading.

The main material of the specimen is a Ytong block. It is a cellular concrete and, therefore, very light that combines resistance and thermal insulation. The main chemical composition of this block is silica sand (70%), cement (14%), blowing agent (0.05%), and also water. The distribution of cells for a block with 500 kg/m^3 of density is macrocells (50%) and microcells (30%) [30]. The minimum compressive strength is 1.5 MPa according to current standards [31].

2.2. Temperature Sensors. The board used in this research has been the Arduino MEGA based on the ATmega328P. It contains everything needed to support the microcontroller; it is simply connected to a computer with a USB cable or powered with an AC-to-DC adapter or battery to get started [32]. The board kept being powered with an AC-to-DC adapter in this research.

Custom sensor expansion boards can be developed to directly plug into the standardized pin-headers of the board. They enable the microcontroller to connect to several sensors [22, 33].

This ensures that power supply will be continuous during the experiment and batteries will not be depleted in several days or weeks.

A program compiled in C++ language has been made for data collection. This program is responsible for data collection, publication, and temperature control inside the test.

The application builds an array of objects, thermometers, which take the temperature, store it, and publish it on both the serial port monitor and HTML by creating a local web server, which allows real-time access to the situation of the test through a local web page.

The structure of the program is based on objects, classes. To do this, it defines a pure virtual class called Thermometer, which defines all common data and methods from acquisition to publication. This main class is inherited by classes that are defined according to different types of sensors, Dallas DS18b20 and K probes, through the MAX 31856 digitalization and amplification module.

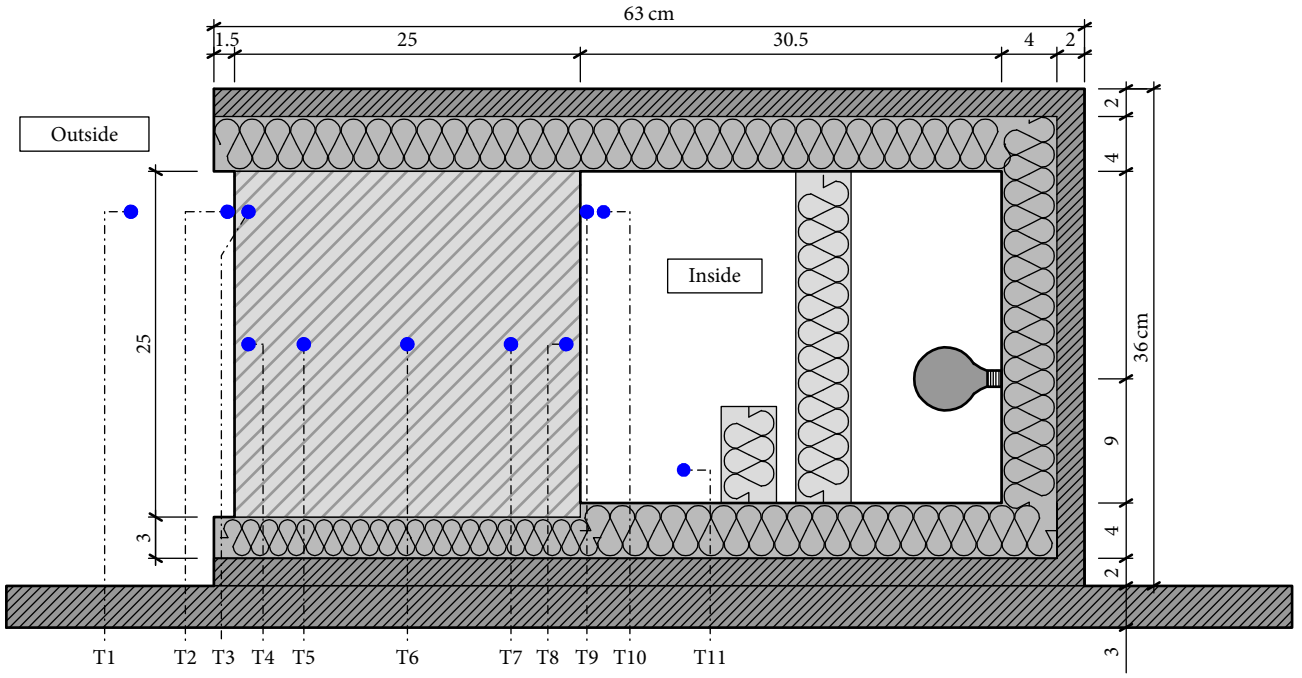

Figure 2: Section of the specimen with the location and sensors nomenclature.

These classes receive the inheritance of the main class, Thermometer. They also define the specific methods of data acquisition according to external libraries of free license. These libraries contain the predefined classes of the specific hardware use of each sensor. There are more than fifty different types of sensor whose deployment into practical devices facilitates long-term monitoring of structural changes, reinforcement corrosion, concrete chemistry, moisture state, and temperature [20]. In this work, only temperature sensors are used.

The Dallas temperature sensor DS18B20 has been used for the main sensors. It can be powered from data line. Power supply range is 3.0 V to 5.5 V. This type of sensor measures temperatures from −55°C to +125°C with ±0.5°C accuracy from −10°C to +85°C. The DS18B20 Digital Thermometer provides 9- to 12-bit (configurable) temperature readings which indicate the temperature of the device. Information is sent to/from the DS18B20 over a 1-Wire interface, so that only one wire (and ground) needs to be connected from a central microprocessor to a DS18B20. Power for reading, writing, and performing temperature conversions can be derived from the data line itself with no need for an external power source. Because each DS18B20 contains a unique silicon serial number, multiple DS18B20s can exist on the same 1-Wire bus. This allows for placing temperature sensors in many different places. Applications where this feature is useful include HVAC environmental controls, sensing temperatures inside buildings, equipment, or machinery, and process monitoring and control [34].

K-type probes have been used to test the data obtained by DS18B20 sensors. These probes can perform measurements below 0°C.

A Dual MAX31856 thermocouple breakout board has been used to connect the K-type temperature sensors to the board. It has 19-bit temperature resolution, handles all thermocouple types (K, J, N, R, S, T, E, and B), and allows readings as high as +1800°C and as low as −210°C depending on thermocouple type, and a line frequency filtering of 50 Hz and 60 Hz is included.

Using a higher resolution external analog-to-digital convertor would provide better readings; however, since the thermistor has an accuracy of ±0.05°C in optimal conditions, the level of precision from the 10-bit ADC is sufficient [19].

In this work, up to 11 temperature sensors have been used. The variations recorded by these sensors over time are known and they are used to corroborate their accuracy and to validate this research. For this reason, all temperature sensors have been calibrated. Calibration is the result of comparing the data obtained by sensors with that obtained by high quality thermometers in a test. In this way, an affordable measurement system can be used in tests, which were previously carried out with expensive thermometers. Calibration has consisted in placing all sensors in a receptacle to test the temperature at different values. The temperature values observed in all thermometers have been very similar. The temperature differences between the sensors and the reference thermometers were lower than ±0.05°C and therefore it was not necessary to correct the data obtained.

Data of all temperature sensors are saved in real time on a micro-SD card in txt format, which can easily be imported into any spreadsheet software. Thus, it is not necessary to connect the sensors to a computer for the long period that the test can last. Micro-SD memory cards that are sold today have a huge storage capacity. Sensor and time data are stored

as plain text in a comma-delimited format and each data point consists of only a few bytes of data, allowing storing billions of measurements [21].

The micro-SD memory card used on the board has been able to store the data received by the 11 sensors, every 5 minutes, for days, and it has no storage problems. A web page has been created to check the temperature of each sensor in real time. However, the web page was very simple and it was not linked to a Mysql database to store these data.

2.3. Thermographic Technology. A FLIR B335 camera has been used for this research generating thermographic images with 320 × 240 pixels of resolution. It has a temperature range between −20 and +120°C and less than 50 mK NETD sensitivity. Further processing of the thermographic images has been done with the FLIR QuickReport software. The colour palette of these pictures can be modified, as well as the temperature range and the distance to the object (usually 1 meter). Also, the maximum, minimum, and average temperature of the studied areas can be calculated. Finally, the temperature assigned to each pixel of the image is exported in Excel format.

The authors have evaluated the contributions on thermal comfort for traditional façades of buildings [35].

Many other previous studies have already established a link between infrared thermography and the detection of defects in stone materials, although in these studies the thermographic data for different points of the walls are interpreted by means of graphs [36]. Those areas where thermal discontinuities occur are usually where defects in the material are located. On the other hand, those points which display a similar temperature demonstrate thermal inertia, that is, the tendency of a particular element to resist thermal changes, and this depends on the characteristics of the material, the moisture present, and any damage [37].

The thermal pattern of a material largely depends on its characteristics (thermal diffusion, porosity, density, etc.). The possibility of being able to clearly visualise the defects of a particular material depends on the difference between the thermal characteristics of the material and the absence of homogeneity [38].

The emissivity value in this study is 0.95 as the default value, and so we believe that the results obtained from the thermographic measurements are reliable. Moreover, emissivity is very similar for nonmetallic materials [39] in building construction. For example, concrete has 0.93 of emissivity, 0.94 for chipboard, or 0.90 for rock wool with a cloth cladding.

2.4. Finite Element Simulation. The research has been completed with a finite element model of the specimen using the commercial program ANSYS Mechanical v.15, a finite element software used in engineering and architecture able to study multiple variables simultaneously [40].

This software allows perfectly simulating the studied case and calculating the thermal flow in each point. For this purpose, a mesh size of 0.5 cm has been used. The element type is Solid 278, a simple three-dimensional parallelepiped of 8 nodes, because it is the element that best fits in the calculations and for the model geometry. The element has a 3D thermal conduction capability. The element has eight nodes with a single degree of freedom, temperature, at each node. The element is applicable to a 3D, steady-state or transient thermal analysis. However, in [41] anyone can see the use of new finite elements for more difficult applications.

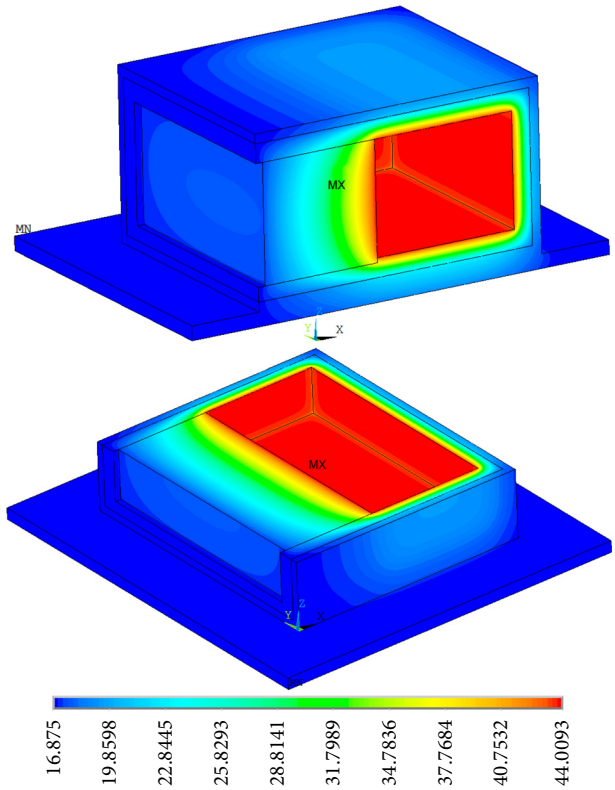

Figure 3: Temperature in the vertical and horizontal section of the finite element model.

Figure 3 shows a vertical section 15 cm from the edge of the three-dimensional model, where the thermometers are located, and a horizontal section through the midpoint. Thus, all elements of the model are best observed. The same materials of the laboratory test (Table 1) have been used in the finite element model. The thermal behaviour of the materials used varies because their properties of density, specific heat, and conductivity are different. Energy is more difficult to propagate when the conductivity of the material is lower. In this case, the lowest conductivity corresponds to rock wool. This way, the energy will be lost more quickly in the concrete block and in the chipboard.

The temperature in all nodes of the finite element mesh (every 0.5 cm) is shown in this figure. Inside the box the heat source raises the temperature 30°C above the outside temperature. Outside, the ambient temperature at the selected time is about 15°C. This generates a temperature gradient between inside and outside. It can be seen very clearly in Figure 3.

A more adequate understanding of the temperature gradient that reflects the finite element model is achieved in this figure.

Table 3: Film coefficients used in the calculations.

Flux ($W/(m^2 \cdot K)$)					
Horizontal		Vertical			
		Upward		Downward	
Out	In	Out	In	Out	In
4	35	4	35	4	35

Figure 3 clearly shows how the thermal gradient occurs through the insulation small thickness of 4 cm. The gradient is wider where the lightweight concrete block is located, considering that its thermal conductivity is higher than the insulation. The temperature decreases along the entire thickness of this material. Also, it is possible to understand more complex physical phenomena by considering the three dimensions, such as the nonlinearity of the thermal gradient of some areas.

The heat exchange between the air and the wall is a complex phenomenon. Each mobile molecule of air strikes the static molecules of the wall material and exchanges with them some of its vibration. Temperature is the mean of the states of vibration.

In the interface between solid and gas, very complex phenomena occur, depending on the air velocity and the horizontal or vertical position of the solid. These phenomena also depend on the temperature of the materials. The balance of these phenomena is simulated rudely by the film coefficient of convention.

The thermography of the solid helps to set the film coefficient, by comparing the temperatures of the simulation with those obtained in the thermography. The heat flow generated by the heat source produces a convection phenomenon of the air inside the box. A heat transfer occurs between the fluid and the surfaces. Here the thermal boundary layer between both elements is very important. This boundary layer is linked with temperature gradients in the fluid caused by the presence of a surface at different temperature. When forced convection occurs, the values of the film coefficient vary between 25 and 70 approximately depending on the air velocity and material, in this case, concrete [42]. In this case, the values of the film coefficient (Table 3) are set to a certain value by comparing the temperature values of the thermography with those of the finite element simulation. Inside the box, the values are higher because the space is very small and the heat source produces a forced convection movement. The values in Table 3 offer a better adjustment of the simulation with the recorded temperatures.

2.5. Validation and Verification (V & V) for Applying in Heritage. The work presented in this paper is based on a specimen carried out in the laboratory with a homogeneous stone material (Figures 1 and 2). It is a chipboard box, totally thermally insulated, except on one of its faces where the solid light concrete block is located. A heat source that generates a thermal gradient is placed in the inner space. Up to 11 temperature sensors are placed in the specimen. It is a low-cost system that allows checking temperatures and storing the data for later analysis.

Once the specimen is set up, the heat source is switched on, in this case, a bulb of 60 W. From that moment, all data generated by the thermal sensors is recorded on an SD card. The test lasted several days, generating a high number of temperature records every five minutes, day and night. Outside temperature has been fluctuating, although the values have been maintained around 15°C inside the laboratory because it was winter. The inside temperature of the housing has also been kept constant with a temperature 30°C above the outside. The T11 thermometer has controlled the bulb's on/off switching. When the temperature difference is not equal to 30°C compared to outside, with a small margin of ±0.5°C, an order is sent to turn the heat source on or off.

In addition, during the experiment, different thermographic pictures were also captured. The temperature of all faces has been recorded from different points of view. This allows comparing temperature data and verifying them more accurately.

A three-dimensional model of the experiment with finite elements was developed to simulate the specimen after obtaining sufficient laboratory data. Data from sensors and thermography has been used to calibrate this 3D theoretical model with finite elements.

The comparison of the data obtained by the three techniques allows validating and verifying (V & V) the theoretical model. Once the finite element model has been validated, it is possible to extrapolate thermal analysis to buildings façades in heritage. An exhaustive check of the temperatures that are reached in different points of a façade can be realized. Extrapolations or modifications in the boundary conditions can be made to know how the material would behave in those suppositions.

After getting the data using the three techniques for the healthy block, three types of damage usual in heritage are applied to the block and the experimental data with sensors and thermal camera are taken again. The variation of these results with respect to the theoretical ones allows detecting the damage. Three types of usual damage on historic buildings façades have been induced in the solid light concrete block.

Damage 1 represents a continuous crack with 0.5 cm of thickness and 5 cm of height and its depth covers the entire thickness of the block (25 cm). Damage 2 involves a mass loss of the material 5 cm in diameter and 10 cm deep from the inner face. Outside of the solid light concrete block nothing is seen with the naked eye. Damage 3 represents a flake, that is, a piece of the block with dimensions of $7.5 \times 15\ cm^2$ which has been detached.

Table 4: Example of data recorded by temperature sensors.

Sensor #	Data	Hour	Temperature (°C)
T01	2017-03-21	11:27:29	16.875
T02	2017-03-21	11:27:29	17.938
T03	2017-03-21	11:27:29	18.375
T04	2017-03-21	11:27:29	18.375
T05	2017-03-21	11:27:29	22.266
T06	2017-03-21	11:27:29	26.313
T07	2017-03-21	11:27:29	34.727
T08	2017-03-21	11:27:29	45.063
T09	2017-03-21	11:27:29	45.122
T10	2017-03-21	11:27:29	45.688
T11	2017-03-21	11:27:29	43.188

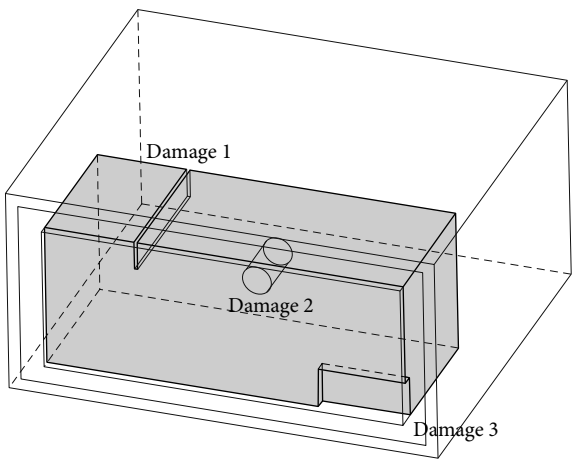

Figure 4: Types of deterioration in the solid light concrete block.

Figure 4 shows the solid light concrete block, with its relative position in the box and with the location of the three damage types.

3. Results and Discussion

3.1. Data Obtained by Temperature Sensors. As explained in the previous section, the micro-SD memory card recorded from the beginning the temperature and the following information: its sensor number, its serial number, the date, time, and whether the heat source is on or off. Table 4 only shows one example, because a large number of data have been stored for days. In the example in Table 4 the T11 thermometer is off.

In Figure 5, the data recorded by the temperature probes in Table 4 are shown.

3.2. Results of Infrared Thermography. In Figure 6, three different points of view have been represented to show the temperatures reached on all the specimen faces. The inside temperature is kept constant at 30°C above the outside temperature.

Figure 7 shows a picture of the specimen and its corresponding thermographic one. The temperature of the central point of the homogeneous material is also shown in this figure. The colour scale allows knowing in a visual way what the temperature degradation of different points of the specimen is.

The methodology carried out in this research is intended to be used in historic buildings. Infrared thermography has been widely used in historic buildings (Figure 8); in this case, it shows the Seminary-School of Corpus Christi of Valencia (Spain), which was built between 1580 and 1610. The façades of this building are composed of a limestone base.

The corners are also reinforced with this type of stone. The main part of the wall is composed of a rammed earth wall. The top of the corner is built with brick. It corresponds with the bell tower. This nondestructive technique is very useful in this type of buildings in heritage. It allows knowing the temperature of inaccessible points with a conventional thermometer and acquiring data from multiple points and detecting injuries and/or humidity.

3.3. Theoretical Results Using the Finite Element Model. The model is calculated when the specimen geometry is entered into the calculation software, the corresponding finite elements are generated, and the relevant boundary conditions are applied. In Figures 3, 9, and 10, we observe the results of the calculation. Before drawing conclusions from the results obtained with the finite element software, the validation work is necessary. Table 5 shows the temperature variation in percentage. The lower value obtained validated these results. Once the model is validated, a large amount of information can be extracted, and extrapolations can be made, modifying some of the parameters involved.

Figure 9 shows the external face of the solid light concrete block. This is a front view. The finite element software allows knowing the temperature in any node of the mesh. The figure shows, as examples, some of the most relevant points: the midpoint, the upper right corner, and two intermediate points. The temperature of the corner (P4) is lower than the midpoint (P1) because it is further away from the heat source.

Table 5 compares the temperatures of the exterior surface of the block obtained by the finite element model and thermography. This table does not show the temperature of the only sensor on this surface, which is 17.938°C.

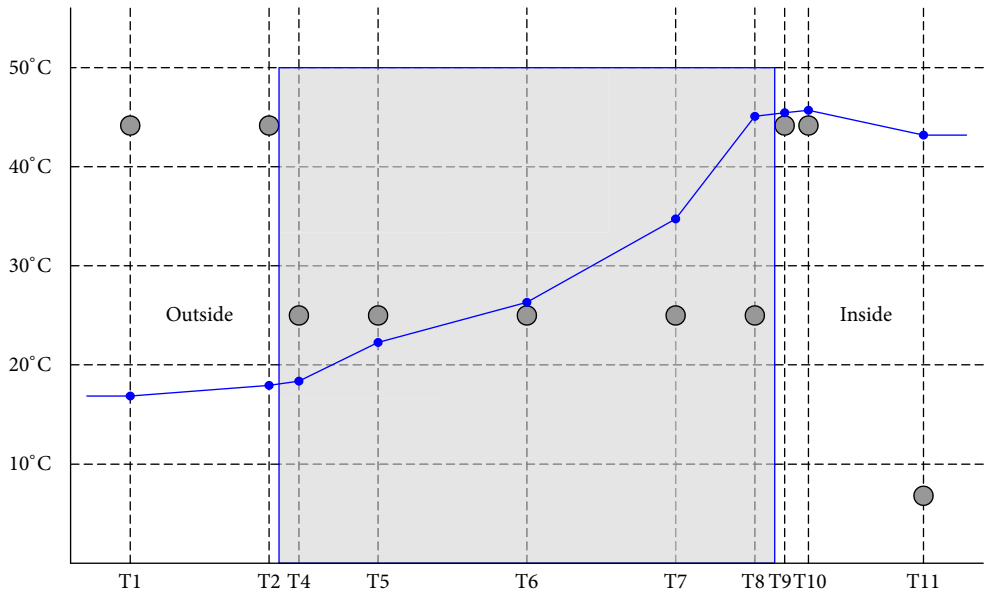

Figure 5: Temperature through the solid light concrete block.

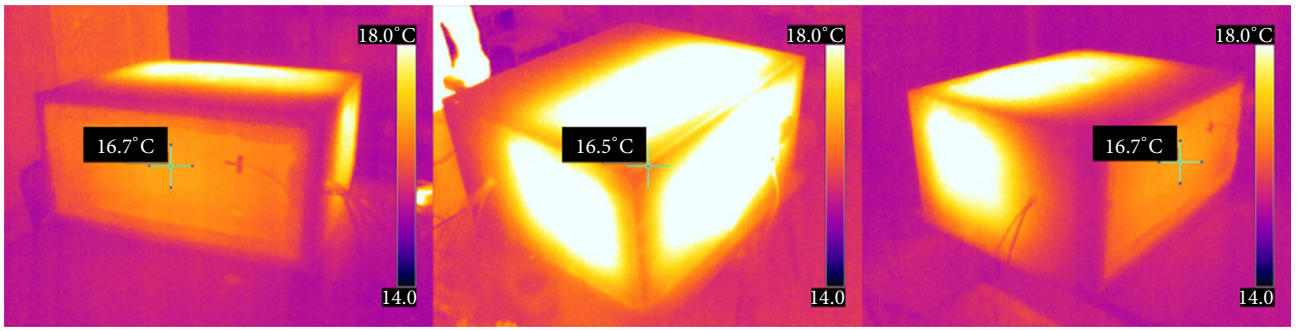

Figure 6: Thermographic pictures from different points of view of the specimen.

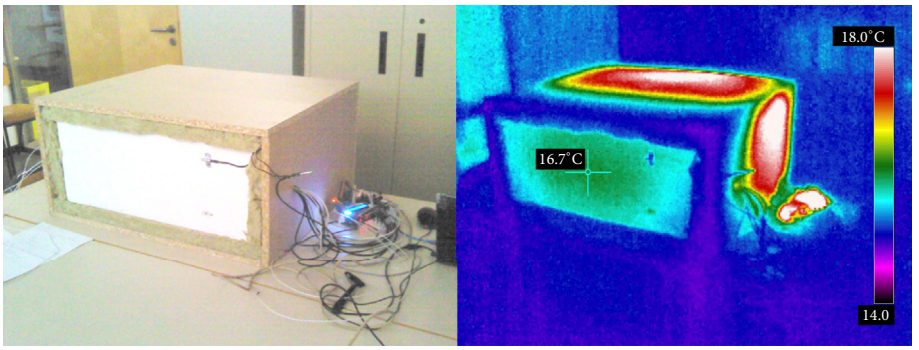

Figure 7: Standard picture and thermography one of the specimen.

In Figure 10, a cross-section of the solid light concrete block is shown. On the left, the outside temperature is 16.875°C. On the right, the inside temperature is 45.688°C that is almost 30°C higher than the outside temperature. The transfer of energy between each face of the solid light concrete block and air through the film coefficient is carried out with about 2°C.

In Figure 10, the five points corresponding to the actual position of the sensors placed in the specimen have been identified. From left to right, they correspond to sensors T04, T05, T06, T07, and T08.

Table 6 compares the temperatures of this section of the block obtained by the sensors and the finite element model. This table does not show the only available temperature

Table 5: Analytical comparison of temperatures obtained on the exterior face of the solid light concrete block, by finite elements and thermography.

Point	Finite elements (°C)	Thermography (°C)	Variation (%)
P1	17.7298	17.8	+0.40%
P2	17.6851	17.9	+1.22%
P3	17.4555	17.5	+0.25%
P4	17.1746	17.2	+0.15%

Table 6: Comparison between theoretical and sensors results.

#	Finite elements (°C)	Sensors (°C)	Variation (%)
T01	16.875	16.875	0.0
T02	18.337	17.938	−2.2
T03	18.466	18.375	−0.5
T04	18.679	18.375	−1.6
T05	22.617	22.266	−1.6
T06	27.668	26.313	−4.9
T07	34.526	34.727	0.6
T08	43.227	45.063	4.2
T09	43.981	43.375	−1.4
T10	45.700	45.688	0.0
T11	—	43.188	—

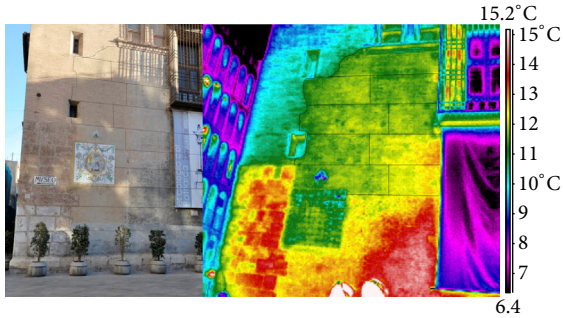

Figure 8: Infrared thermography applied to a historic building.

data of the thermography, that is, 17.9°C. There is a good correspondence between the results obtained by these two techniques.

3.4. Heritage Pathology Detection. Once the block has been damaged, the data storage is carried out again. This is in a later time, when the outside temperature is different. Due to this, it is necessary to simulate the theoretical model again with the new boundary conditions and to make new thermographic captures.

Sensors give temperatures in the depth of the block while the thermography takes its superficial data. Both aspects should be studied by comparing them with the theoretical data. Table 7 shows the results of the sensors and in Table 8 the results of the thermography are shown.

When the solid light concrete block is damaged, the inner temperature goes outwards more easily creating a thermal bridge. This is the main conclusion drawn from Table 7. The thermometers at the edge of the block (T4 and T8) reach a small temperature variation at shallow depth. However, the thermometers in the middle of the block (T5, T6, and T7) recorded a very significant temperature increase, about 17%. When the actual data are significantly different from the theoretical ones it is demonstrated that the areas with pathology are identified.

Figure 11 shows the thermographic pictures with the three damaged zones (a, b, and c) in solid light concrete block. It indicates the temperature in each zone where they are located.

Table 8 compares the temperatures of the theoretical healthy case (finite elements) with the thermography ones for the case of the solid light concrete block with damage. The temperatures obtained at these damaged points are significantly higher. A 19.5% of variation is observed in the case of a crack that crosses the entire thickness of the façade (type 1). However, the mass loss in the middle part of the block (type 2) or a detachment (type 3) increases the temperature less than 10%. This shows that pathologies are detected using this methodology and defects that cross the entire thickness of the wall are more significant in terms of their thermal behaviour.

4. Conclusions

Thermal behaviour of building façades and heat losses through them must be known. The study of the influence of these energy flows, along with other environmental and climatological factors in the deterioration of the façades, is important. This is crucial in heritage, where buildings have suffered for centuries the inclement weather and their façades

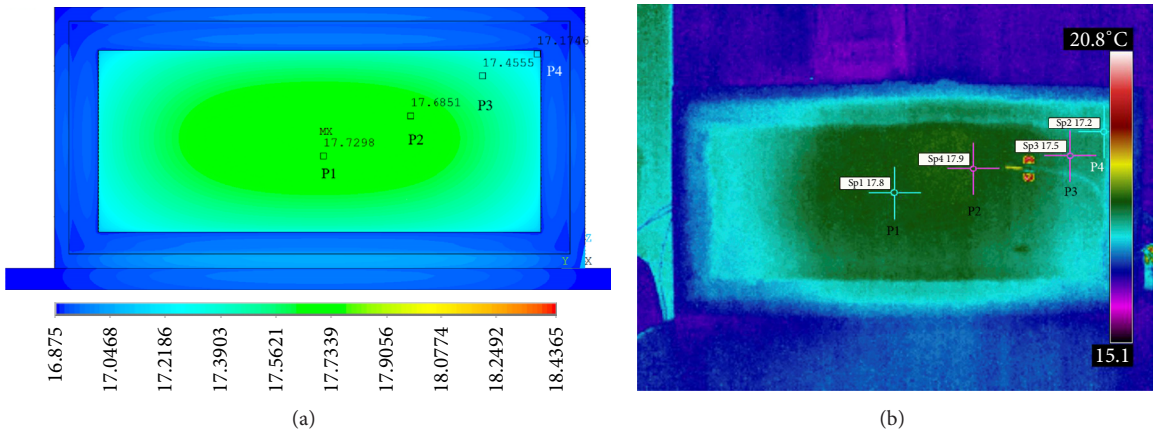

(a) (b)

Figure 9: Temperatures comparison on the exterior surface of the solid light concrete block, by finite elements (a) and thermography (b).

Table 7: Comparison between theoretical and sensors results in damaged block.

Sensor #	Healthy block finite elements (°C)	Damaged block sensors temperature (°C)	Variation (%)
T01	17.500	17.500	+0.0
T02	18.597	19.313	+3.9
T03	19.259	20.125	+4.5
T04	19.433	20.188	+3.9
T05	23.696	27.719	**+17.0**
T06	29.370	33.438	**+13.9**
T07	36.124	42.141	**+16.7**
T08	45.368	49.625	+9.4
T09	46.912	50.375	+7.4
T10	47.500	50.000	+5.3
T11	—	47.313	—

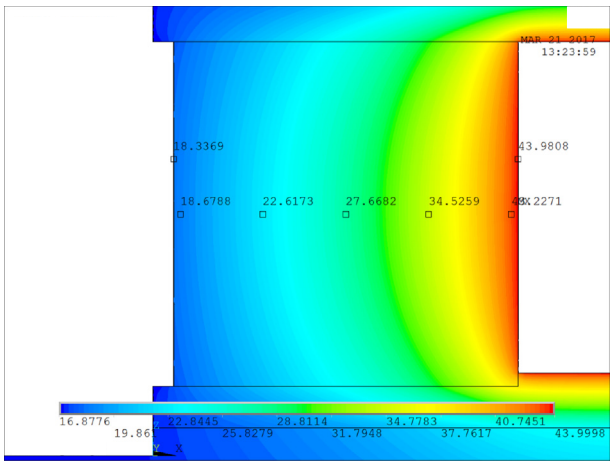

Figure 10: Temperature in the section of the solid light concrete block.

have lasted as long as possible. Most of these historic buildings are composed of façades of a homogeneous material, usually stone, but they can also be made of rammed earth or brick.

With the aim of applying this methodology in façades of historic buildings, the following conclusions can be highlighted:

(a) Thanks to this methodology, it is possible to understand more complex physical phenomena by considering the three dimensions, such as the nonlinearity of the thermal gradient of some areas. When performing the 3D study instead of the 2D one, the real boundary conditions are analysed and all aspects involved in the thermal behaviour at each point are considered.

(b) This methodology allows detecting damage in buildings. This damage is localized when a considerable variation appears between the theoretical results (finite elements) and the experimental ones (thermal sensor and thermal camera) in some area of the façade. Damage is located generally with a thermal bridge, that is, an area with higher temperatures than expected, because when there is some damage the section is depleted and the heat goes out to the outside more easily by this zone.

(c) Accuracy of film coefficient values is essential for obtaining results in line with reality in thermal simulation programs. Infrared thermography is a very

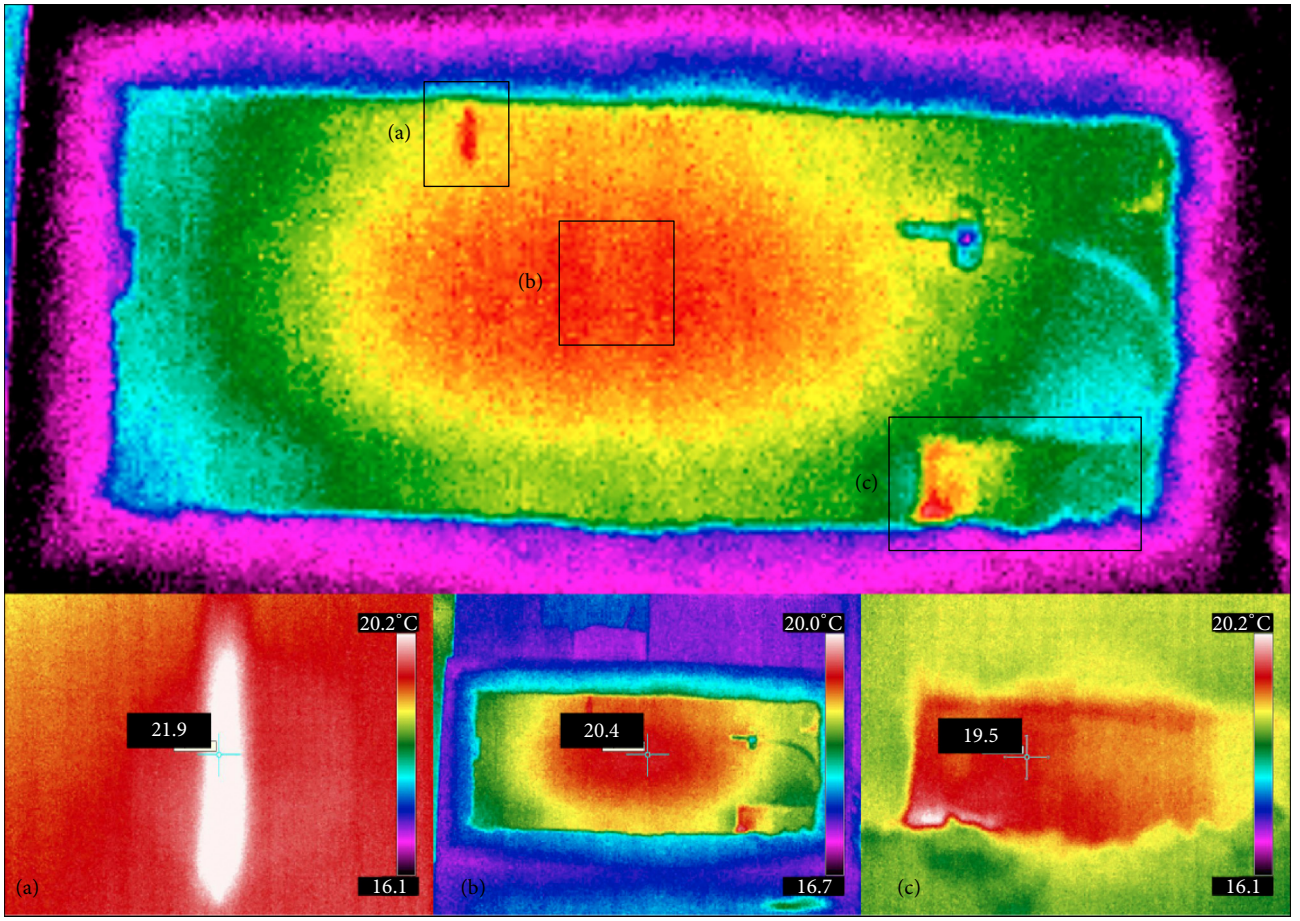

Figure 11: Thermography of the solid light concrete block with damage: (a) type 1, (b) type 2, and (c) type 3.

Table 8: Comparison of the theoretical temperatures and thermographies.

Damage type	Healthy block finite elements (°C)	Damaged block thermography (°C)	Variation (%)
1	18.3286	21.9	**+19.5**
2	18.6333	20.4	+9.5
3	18.1529	19.5	+7.4

useful tool to calibrate the different film coefficient values in a building, and from these, the simulation can be done and results and conclusions of all its points can be extracted.

(d) This research has shown that it is possible and very useful to design the Arduino-based software and hardware necessary to place 11 or even more temperature probes on the same board. In addition, it is possible to store this information during the days or weeks for which the specimen has lasted. This is a very powerful and economical tool for preventive conservation.

(e) Thermal insulation produces a more pronounced thermal gradient due to its thermal conductivity. Meanwhile, the gradient widens in the thickness of the solid light concrete block.

(f) The software allows showing the temperature flows through the different materials. In this way, to find out in which areas the largest flows have originated is possible and, therefore, the greatest energy losses are known. This is vitally important for the objective pursued in this research. Specifically, the greatest energy losses have occurred at the corners of the interior space where the heat source is located.

Conflicts of Interest

The authors declare that there are no conflicts of interest regarding the publication of this paper.

References

[1] G. Pérez, J. Coma, I. Martorell, and L. F. Cabeza, "Vertical Greenery Systems (VGS) for energy saving in buildings: a review," *Renewable and Sustainable Energy Reviews*, vol. 39, pp. 139–165, 2014.

[2] E. Schettini, I. Blanco, C. A. Campiotti, C. Bibbiani, F. Fantozzi, and G. Vox, "Green Control of Microclimate in Buildings," *Agriculture and Agricultural Science Procedia*, vol. 8, pp. 576–582, 2016.

[3] R. W. F. Cameron, J. E. Taylor, and M. R. Emmett, "What's 'cool' in the world of green façades? How plant choice influences the cooling properties of green walls," *Building and Environment*, vol. 73, pp. 198–207, 2014.

[4] B. A. Norton, A. M. Coutts, S. J. Livesley, R. J. Harris, A. M. Hunter, and N. S. G. Williams, "Planning for cooler cities: A framework to prioritise green infrastructure to mitigate high temperatures in urban landscapes," *Landscape and Urban Planning*, vol. 134, pp. 127–138, 2015.

[5] U. Berardi, A. GhaffarianHoseini, and A. GhaffarianHoseini, "State-of-the-art analysis of the environmental benefits of green roofs," *Applied Energy*, vol. 115, pp. 411–428, 2014.

[6] R. Fernandez-Ca, T. Emilsson, C. Fernandez-Barba, M. A. Herrera Machuca, and R. Fernandez-Cañero, "Green roof systems: a study of public attitudes and preferences in southern Spain," *Journal of Environmental Management*, vol. 128, pp. 106–115, 2013.

[7] R. A. Francis and J. Lorimer, "Urban reconciliation ecology: the potential of living roofs and walls," *Journal of Environmental Management*, vol. 92, no. 6, pp. 1429–1437, 2011.

[8] B. Raji, M. J. Tenpierik, and A. Van Den Dobbelsteen, "The impact of greening systems on building energy performance: a literature review," *Renewable and Sustainable Energy Reviews*, vol. 45, pp. 610–623, 2015.

[9] O. Guerra-Santin and C. A. Tweed, "In-use monitoring of buildings: an overview of data collection methods," *Energy and Buildings*, vol. 93, pp. 189–207, 2015.

[10] T. Babaei, H. Abdi, C. P. Lim, and S. Nahavandi, "A study and a directory of energy consumption data sets of buildings," *Energy and Buildings*, vol. 94, pp. 91–99, 2015.

[11] J. Langevin, J. Wen, and P. L. Gurian, "Simulating the human-building interaction: Development and validation of an agent-based model of office occupant behaviors," *Building and Environment*, vol. 88, pp. 27–45, 2015.

[12] J. B. Siviour, "Experimental U-values of some house walls," *Building Services Engineering Research & Technology*, vol. 15, no. 1, pp. 35-36, 1994.

[13] S. Doran, "Improving the thermal performance of buildings in practice, in: BREClient Report No. 78132, for the Office of the Deputy Prime Minister," Tech. Rep., Building Research Establishment, Glasgow, Scotland, 2005.

[14] H. Hens, A. Janssens, W. Depraetere, J. Carmeliet, and J. Lecompte, "Brick cavity walls: A performance analysis based on measurements and simulations," *Journal of Building Physics*, vol. 31, no. 2, pp. 95–124, 2007.

[15] N. Barroca, L. M. Borges, F. J. Velez, F. Monteiro, M. Górski, and J. Castro-Gomes, "Wireless sensor networks for temperature and humidity monitoring within concrete structures," *Construction and Building Materials*, vol. 40, pp. 1156–1166, 2013.

[16] A. K. Das, A. Haldar, and S. Chakraborty, "Health assessment of large two dimensional structures using limited information: recent advances," *Advances in Civil Engineering*, vol. 2012, Article ID 582472, 16 pages, 2012.

[17] P. Merello, F.-J. García-Diego, and M. Zarzo, "Diagnosis of abnormal patterns in multivariate microclimate monitoring: A case study of an open-air archaeological site in Pompeii (Italy)," *Science of the Total Environment*, vol. 488-489, no. 1, pp. 14–25, 2014.

[18] F.-J. García Diego, B. Esteban, and P. Merello, "Design of a hybrid (wired/wireless) acquisition data system for monitoring of cultural heritage physical parameters in smart cities," *Sensors (Switzerland)*, vol. 15, no. 4, pp. 7246–7266, 2015.

[19] N. Buenfeld, R. Davis, A. Karmini, and A. Gilbertson, *Intelligent Monitoring of Concrete Structures*, CIRIA, London, UK, 666th edition, 2008.

[20] W. J. McCarter and O. Vennesland, "Sensor systems for use in reinforced concrete structures," *Construction and Building Materials*, vol. 18, no. 6, pp. 351–358, 2004.

[21] A. S. Ali, Z. Zanzinger, D. Debose, and B. Stephens, "Open Source Building Science Sensors (OSBSS): A low-cost Arduino-based platform for long-term indoor environmental data collection," *Building and Environment*, vol. 100, pp. 114–126, 2016.

[22] S. Ferdoush and X. Li, "Wireless sensor network system design using raspberry Pi and Arduino for environmental monitoring applications," in *Proceedings of the The 9th International Conference on Future Networks and Communications (FNC'2014)/The 11th International Conference on Mobile Systems and Pervasive Computing (MobiSPC'14)*, vol. 34, pp. 103–110, Ontario, Canada, 2014.

[23] S. Hicks, A. K. Aufdenkampe, and D. S. Montgomery, "Creative uses of custom electronics for environmentalmonitoring," in *Proceedings of the American Geophysical Union Annual Fall Meeting*, San Francisco, Calif, USA, December, 2012.

[24] A. Kruger, J. J. Niemeier, and D. L. Ceynar, "The drifter platform for measurements in small rivers," in *Proceedings of the American Geophysical Union Annual Fall Meeting*, San Francisco, Calif, USA, December, 2011.

[25] P. Queloz, J. Besuchet, P. S. C. Rao, and A. Rinaldo, "Development of a low-cost Wireless controller for flexible sampling strategies based on real-time flow monitoring," in *Proceedings of the EGU General Assembly Conference*, Vienna, Austria, 2013.

[26] F. Mercuri, U. Zammit, N. Orazi, S. Paoloni, M. Marinelli, and F. Scudieri, "Active infrared thermography applied to the investigation of art and historic artefacts," *Journal of Thermal Analysis and Calorimetry*, vol. 104, no. 2, pp. 475–485, 2011.

[27] C. Lerma, Á. Mas, E. Gil, J. Vercher, and M. J. Peñalver, "Pathology of Building Materials in Historic Buildings. Relationship Between Laboratory Testing and Infrared Thermography," *Materiales de Construcción*, vol. 64, no. 313, p. e009, 2014.

[28] E. Barreira, R. M. Almeida, and M. Moreira, "An infrared thermography passive approach to assess the effect of leakage points in buildings," *Energy and Buildings*, vol. 140, pp. 224–235, 2017.

[29] E. Barreira, R. M. S. F. Almeida, and J. M. P. Q. Delgado, "Infrared thermography for assessing moisture related phenomena in building components," *Construction and Building Materials*, vol. 110, pp. 251–269, 2016.

[30] Ytong. Guía técnica. El hormigón celular YTONG, material de construcción. http://www.ytong.es/es/docs/GuiaTecnica_Ytong_2014.pdf. Visited on 2017-02-17.

[31] AENOR, Specification for masonry units. Part 4: Autoclaved aerated concrete masonry units (UNE-EN 771-4) 2016.

[32] Arduino Platform. https://www.arduino.cc/en/Main/ArduinoBoardUno.

[33] R. Hut, *New Observational Tools and Data Sources for Hydrology: Hydrological Data Unlocked by Tinkering (Master thesis [Master, thesis]*, Delft University of Technology, Amsterdam, Netherlands, 2013.

[34] Dallas Semiconductor https://www.maximintegrated.com/en/products/analog/sensors-and-sensor-interface/DS18B20.html.

[35] J. Vercher, F. Cubel, C. Lerma, Á. Mas, E. Gil, and Á. Mas, *Contributions of traditional façades to the thermal comfort. Earthen Architecture: Past, Present and Future*, Taylor & Francis Group, Park Drive, UK, 2015.

[36] M. Danese, U. Demšar, N. Masini, and M. Charlton, "Investigating material decay of historic buildings using visual analytics with multi-temporal infrared thermographic data," *Archaeometry*, vol. 52, no. 3, pp. 482–501, 2010.

[37] J. B. Campbell, *Introduction to Remote Sensing*, Taylor & Francis, London, UK, 2nd edition, 1996.

[38] C. Meola, G. M. Carlomagno, and L. Giorleo, "The use of infrared thermography for materials characterization," *Journal of Materials Processing Technology*, vol. 155-156, no. 1-3, pp. 1132–1137, 2004.

[39] I. Cañas, S. Martin, and I. González, "Thermal-physical aspects of materials used for the construction or rural buildings in Soria (Spain)," *Construction & Building Materials*, vol. 19, pp. 197–211, 2005, http://dx.doi.org/10.1016/j.conbuildmat.2004.05.016.

[40] Ansys. 2013. Ansys 15.0 Help Manual. Ansys Inc. Ansys Academic Research V15.0. USA.

[41] V. A. Eremeyev, A. Skrzat, and F. Stachowicz, "On finite element computations of contact problems in micropolar elasticity," *Advances in Materials Science and Engineering*, vol. 2016, Article ID 9675604, 9 pages, 2016.

[42] J. Chávez-Galán, R. Almanza, and C. N. Rodríguez, "Convective heat transfer coefficients: experimental estimation and its impa ct on thermal building design for walls made of different Mexican building materials," *Concreto y Cemento. Investigación y Desarrollo*, vol. 5, no. 2, pp. 26–38, 2014.